X-822

EXTERNAL TRANSMITTAL
AUTHORIZED

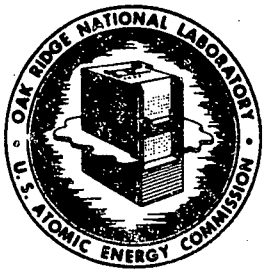

OAK RIDGE NATIONAL LABORATORY
Operated by
UNION CARBIDE NUCLEAR COMPANY
Division of Union Carbide Corporation
UCC
Post Office Box X
Oak Ridge, Tennessee

ORNL
CENTRAL FILES NUMBER
CF-58-7-76

COPY NO. 138

DATE: July 28, 1958

SUBJECT: Survey of the Static Nuclear Characteristics of Small, One-Region Slurry Reactors.

TO: HRP Distribution

FROM: B. E. Prince and M. W. Rosenthal

ABSTRACT

Survey calculations were made of the criticality characteristics of some small one-region thorium-oxide slurry reactors. Fuels considered were U^{235} and U^{233}, and both D_2O and H_2O moderated systems were studied. Critical fuel concentrations were calculated as functions of size, temperature, and thorium concentration. For 4- to 5 1/2-ft diameter spherical ThO_2-D_2O reactors fueled with U^{235}, the minima in the U^{235}/Th ratio curves occurred at about 200 gm Th/liter. The critical ratio obtained for a 5-ft diameter bare D_2O reactor at 280°C increased from 0.08 to 0.10 g U^{235}/g Th as the thorium concentration was increased from 200 to 400 gms per liter.

DISCLAIMER

SUMMARY

A survey was made of the static nuclear characteristics of some small one-region thorium-oxide slurry reactors. Fuels considered were U^{235} and U^{233} (isotopically pure), and both D_2O and H_2O moderated systems were studied. In all cases the reactors were assumed to be free of poisons. Moderator absorptions were neglected for D_2O and were assumed for H_2O to be those of the pure moderator at temperature. The computations were performed on the Oracle, using a modified Fermi age, bare reactor model, which allowed for resonance absorptions in fuel.

Critical fuel concentrations are shown graphically as a function of size, temperature, and thorium concentration. Temperature coefficients of reactivity for several of the reactors are tabulated. Comparison with more exact calculations and application of the numerical results to actual pressure-vessel enclosed reactors is discussed. Some of the results are used to examine the changes in criticality conditions resulting from uniform changes in slurry concentration.

For 3 to 5-ft diameter ThO_2 - D_2O spherical reactors fueled with U^{235}, the minima in the critical-mass-ratio curves (gms U^{235}/gm Th) occurs at about 200 gm Th/liter. In H_2O reactors of the same diameter, the critical mass ratio continues to decrease up to 600 th Th/liter. For example, the critical mass ratio of a 5-ft diameter U^{235} - D_2O reactor at 280°C varies from 0.08 to 0.10 as the thorium concentration is increased from 200 to 400 gm/liter. In an H_2O moderated reactor of the same size and temperature, this ratio decreases from 0.076 to 0.046 for the same change in thorium concentration.

RESULTS

The range of reactor parameters studied is listed in Table I. For the U^{235} and U^{233}-fueled, D_2O-moderated reactors, the critical concentrations are plotted vs. size, temperature, and thorium concentration in Figures 1 to 4. The corresponding results for the U^{235} fueled, H_2O moderated systems are given in Figures 5 to 8. In the same order, Figures 9 to 16 summarize the criticality characteristics of the U^{233} fueled reactors. Reactivity temperature coefficients of several of the reactors are given in Table II for the case of spatially uniform heating in which the ratios of fuel and thorium to moderator remain constant. The temperature coefficient is approximately equal to the sum of the individual leakage coefficients of reactivity associated with changes in temperature.

Table I: Range of Parameters Studied

Fuel	U^{235}, U^{233}
Moderator	D_2O, H_2O
Diameter of bare sphere, ft	3 - 5 1/2
Temperature, ^oC	20 - 300
Thorium concentration, g/liter	0 - 600

Table II: Temperature Coefficients of Reactivity

Moderator	Temp. (°C)	Diam. of Bare Sphere (ft)	Thorium Concentration (g/l)	Fast Lkg. Coeff. x 10^{+3} $(°C)^{-1}$	Thermal Lkg. Coeff. x 10^{+3} $(°C)^{-1}$	$\frac{1}{k}\frac{dk}{dT}$ x 10^{+3} $(°C)^{-1}$
D_2O	250	4	200	- 2.04	- .29	- 2.33
		5	200	- 1.30	- .52	- 1.82
			500	- 1.30	- .18	- 1.48
	280	4	200	- 2.84	- .10	- 2.94
		5	200	- 1.82	- .58	- 2.40
H_2O	250	4	200	- .44	- .10	- .54
			500	- .44	- .08	- .52
		5	200	- .30	- .07	- .37
			500	- .30	- .06	- .36
	280	4	200	- .67	- .14	- .81
			500	- .67	- .11	- .78
		5	200	- .45	- .09	- .54
			500	- .45	- .07	- .52

DISCUSSION OF RESULTS

Although the computations of this survey were performed for bare spheres,* the pressure shell will actually serve as a neutron reflector; thus the actual I.D. of the shell will be reduced by a small amount from the bare reactor with the same critical concentration. In order to estimate this size correction, and also to check the validity of some of the assumptions used in the simplified model, criticality in several U^{235}-D_2O reactors was calculated using a multi-group neutron diffusion program. These computations were performed on the

* The corresponding sizes for bare cylinders may be obtained by equating the geometric bucklings of the reactors.

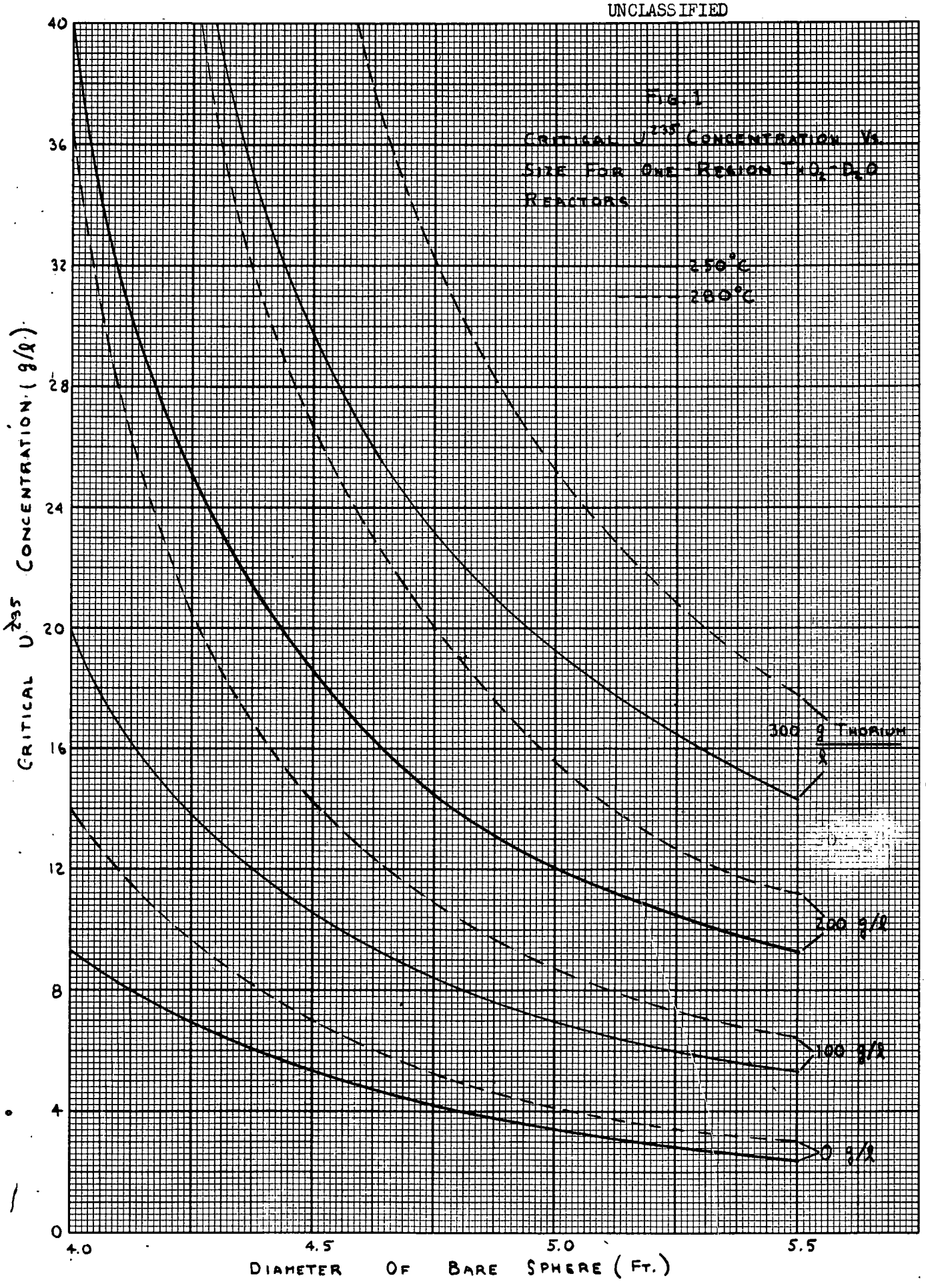
FIG. 1
CRITICAL U235 CONCENTRATION VS. SIZE FOR ONE-REGION ThO2-D2O REACTORS
250°C
280°C
300 g/l THORIUM
200 g/l
100 g/l
0 g/l
CRITICAL U235 CONCENTRATION (g/l)
DIAMETER OF BARE SPHERE (FT.)
0
4
8
12
16
20
24
28
32
36
40
4.0
4.5
5.0
5.5

ORNL-LR-Dwg.-32406
UNCLASSIFIED

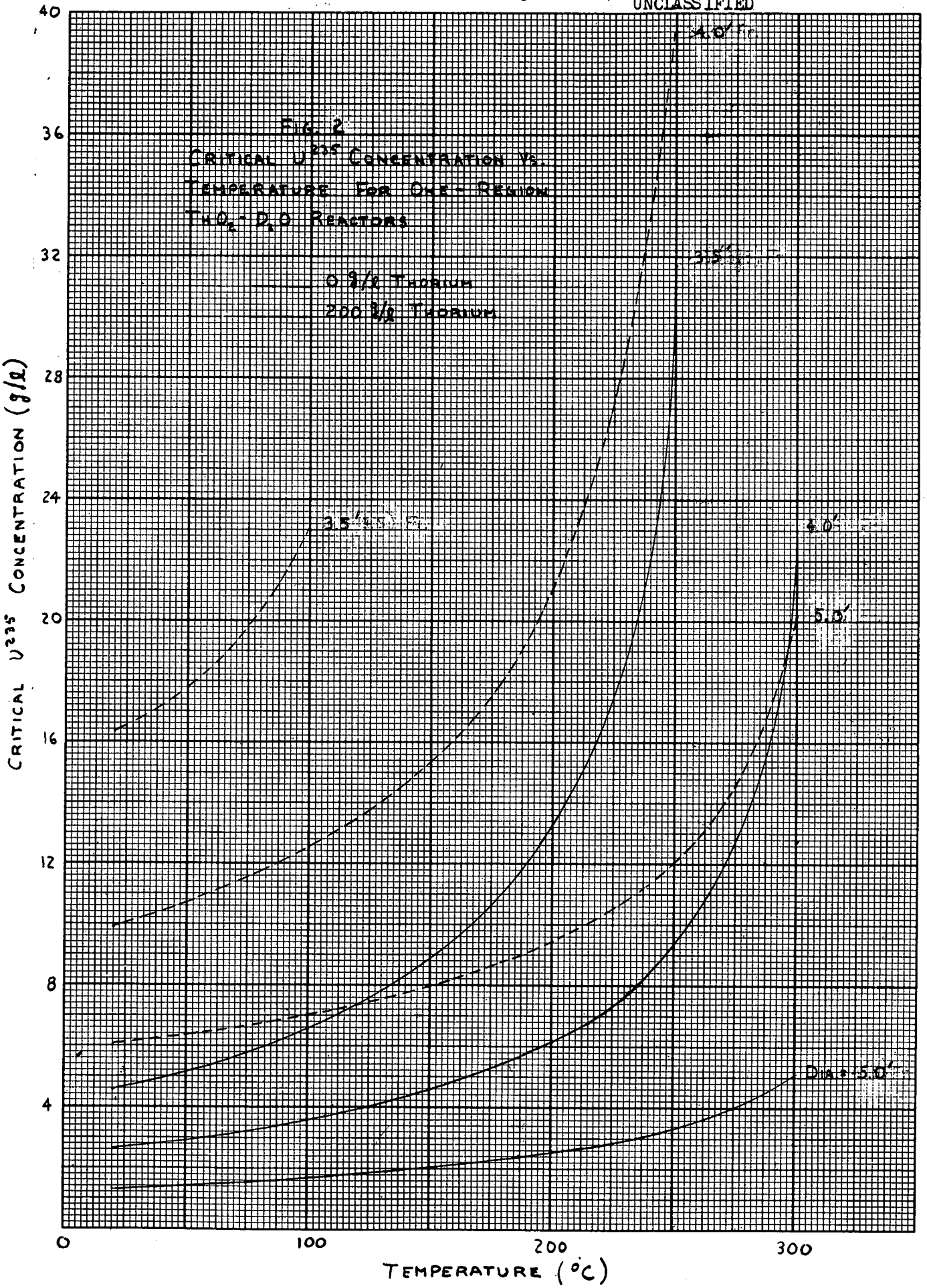

Fig. 2
Critical U^{235} Concentration vs. Temperature for One-Region ThO_2-D_2O Reactors

ORNL-LR-Dwg.-32407
UNCLASSIFIED

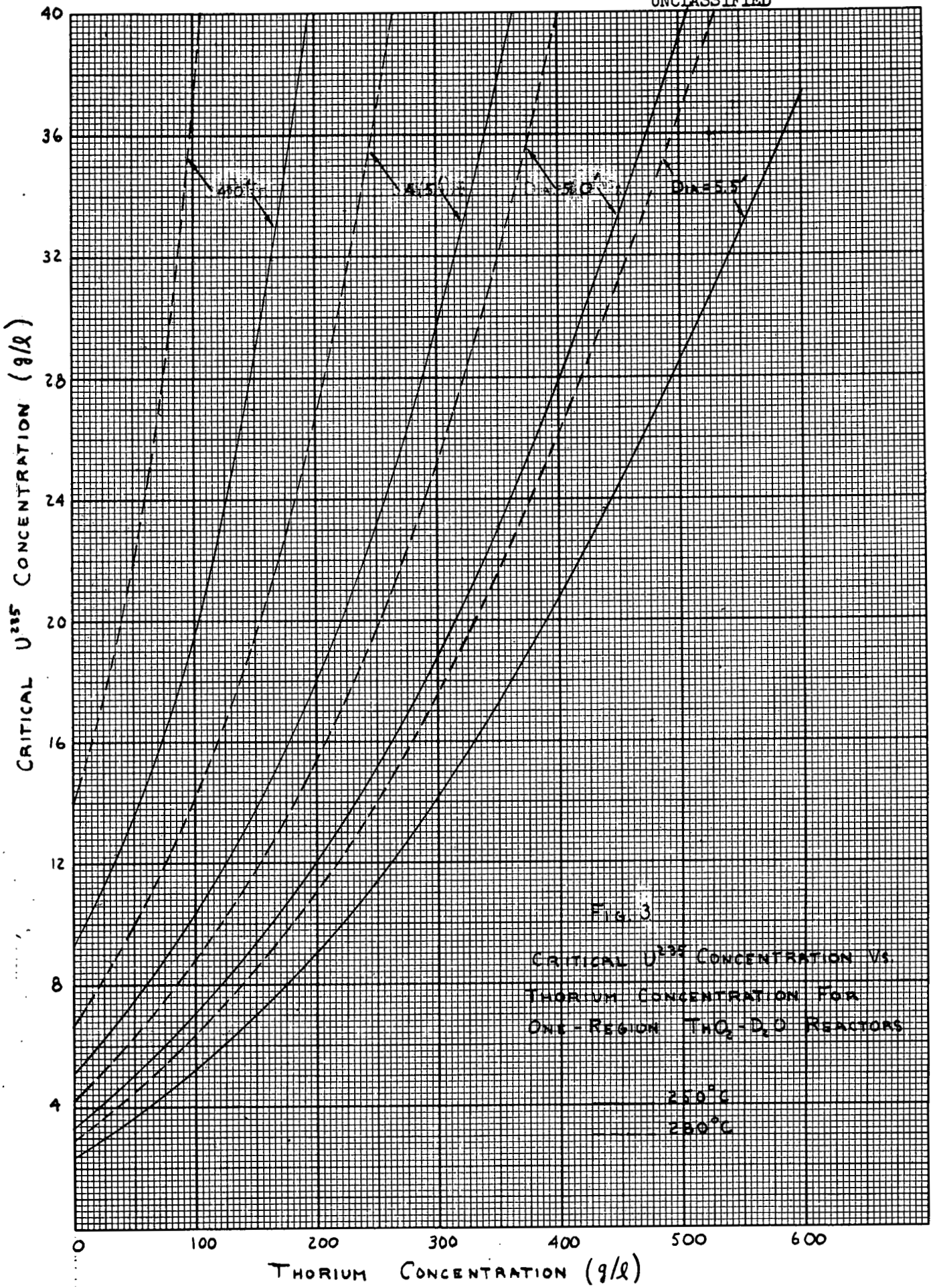

Fig. 3

CRITICAL U^{235} CONCENTRATION VS. THORIUM CONCENTRATION FOR ONE-REGION ThO_2-D_2O REACTORS

ORNL-LR-Dwg.-32408
UNCLASSIFIED

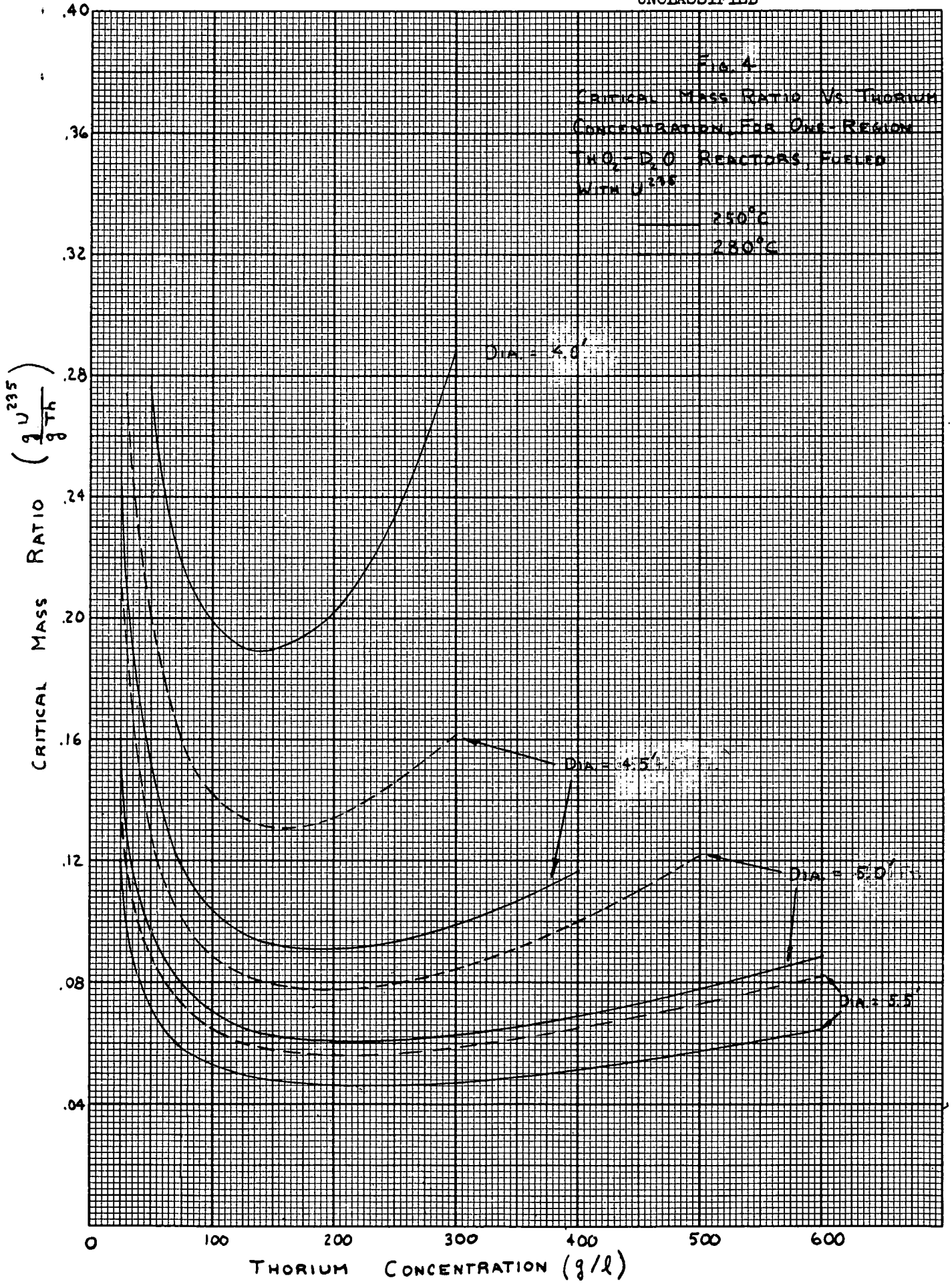

ORNL-LR-Dwg.-32409
UNCLASSIFIED

FIG. 5
CRITICAL U^{235} CONCENTRATION VS. SIZE FOR ONE-REGION ThO_2 - H_2O REACTORS

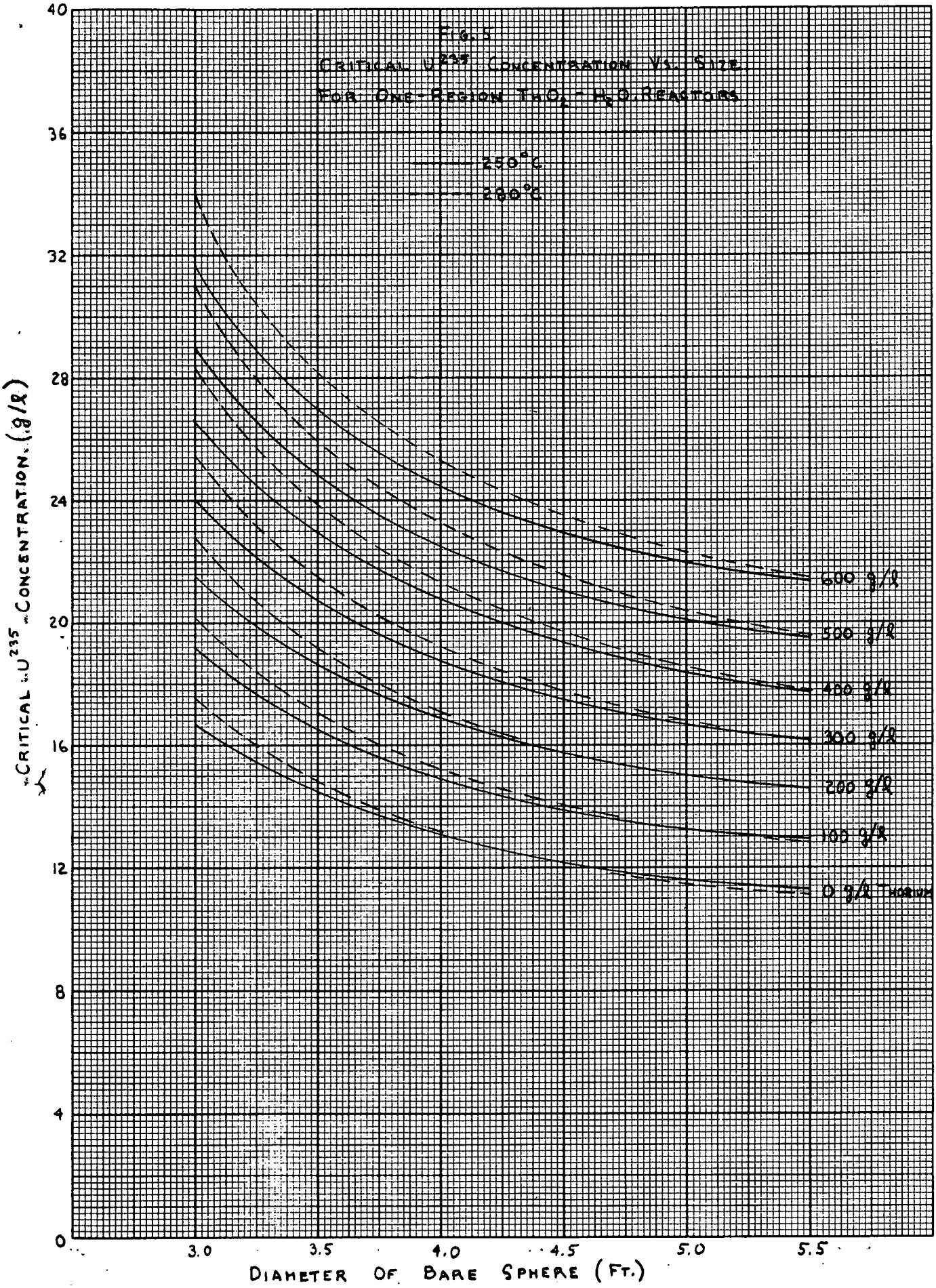

ORNL-LR-Dwg.-32410
UNCLASSIFIED

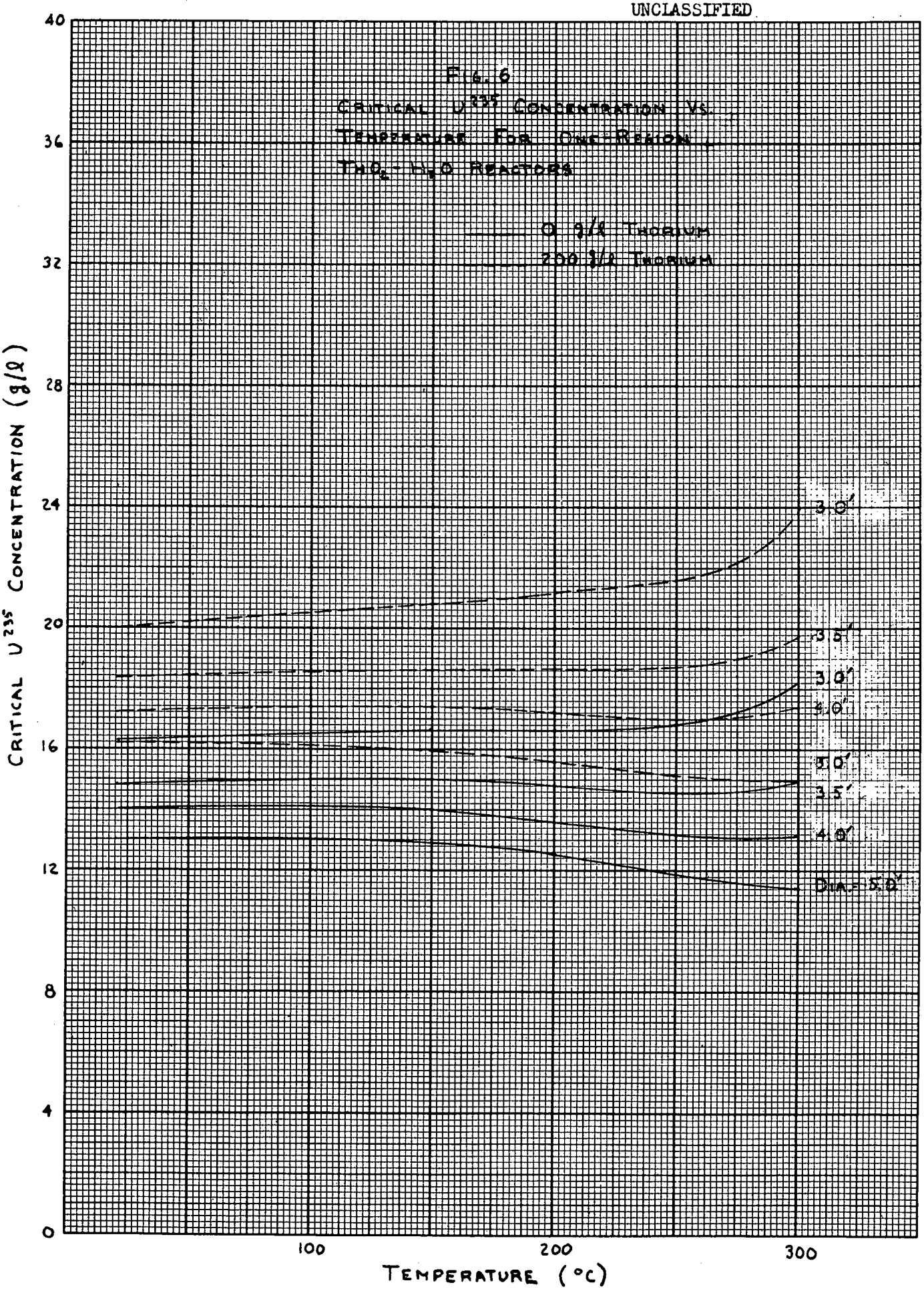

ORNL-LR-Dwg.-32411
UNCLASSIFIED

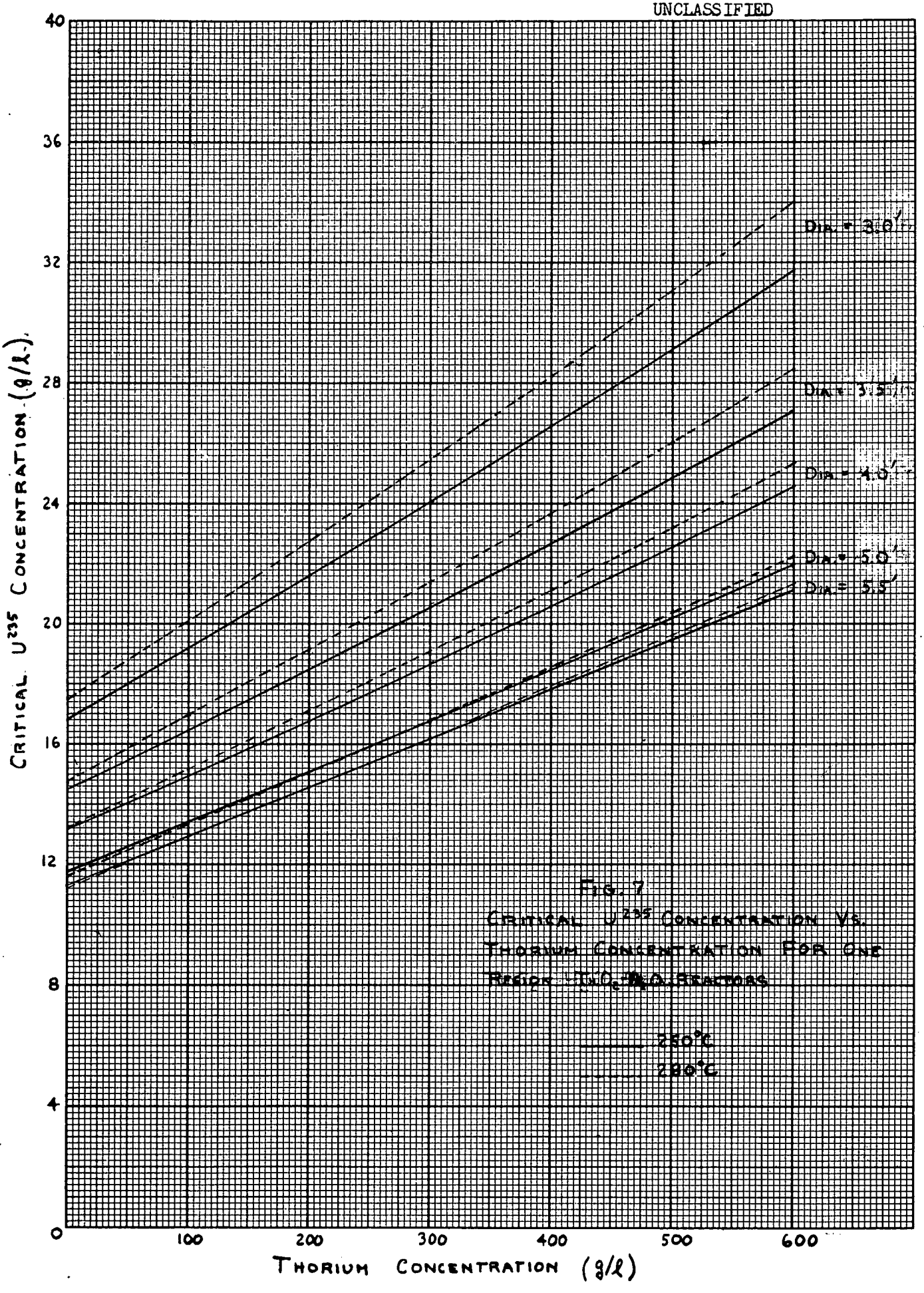

Fig. 7
Critical U^{235} Concentration Vs. Thorium Concentration For One Region ThO_2-UO_2 Reactors.

——— 250°C.
– – – – 280°C.

ORNL-LR-Dwg.-32412
UNCLASSIFIED

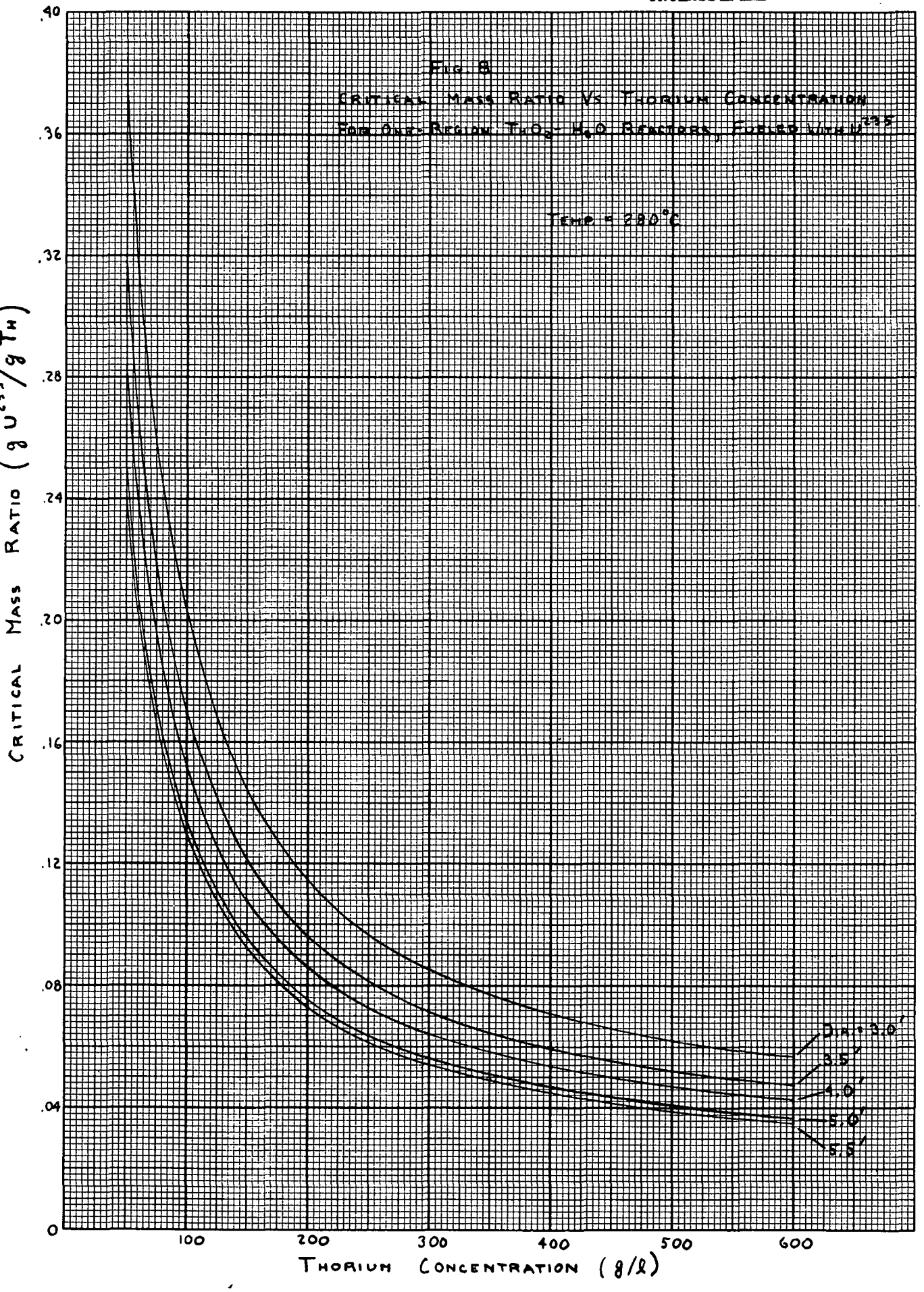

ORNL-LR-Dwg.-32413
UNCLASSIFIED

FIG. 9
CRITICAL U^{233} CONCENTRATION VS. SIZE
FOR ONE-REGION ThO_2-D_2O REACTORS

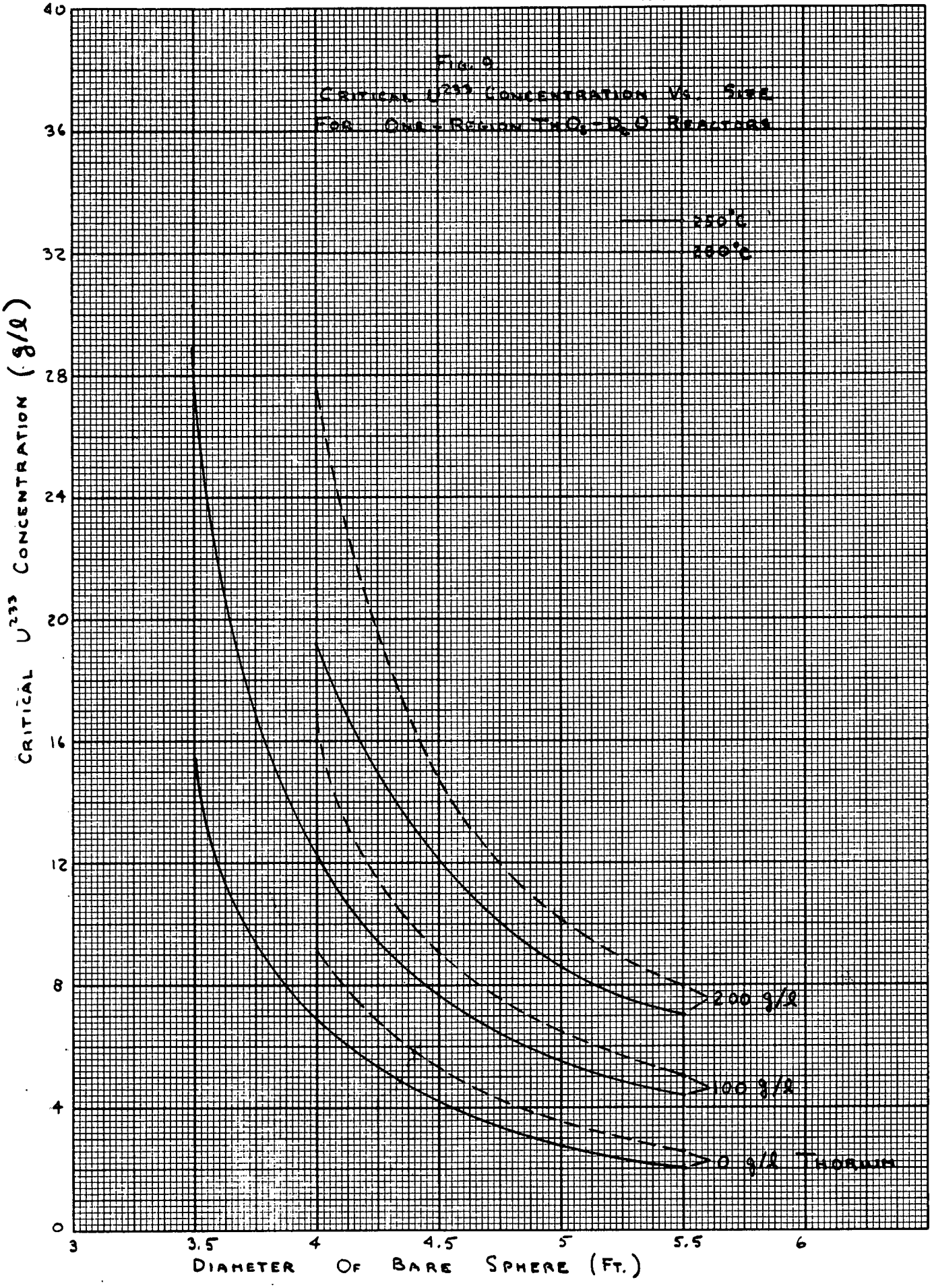

ORNL-LR-Dwg.-32414
UNCLASSIFIED

FIG. 110
CRITICAL U^{233} CONCENTRATION VS. TEMPERATURE FOR ONE-REGION ThO_2-D_2O REACTORS

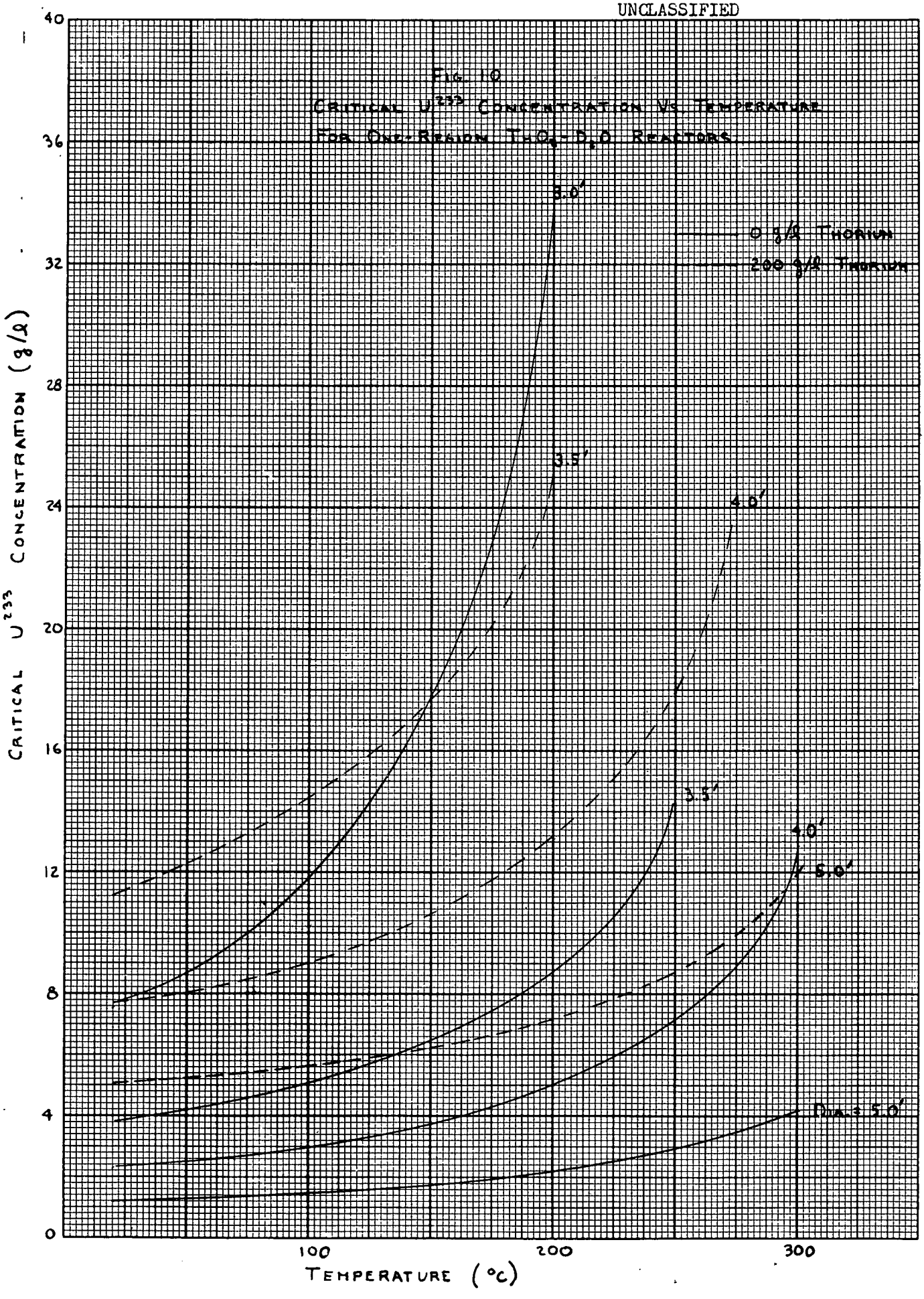

ORNL-LR-Dwg.-32415
UNCLASSIFIED

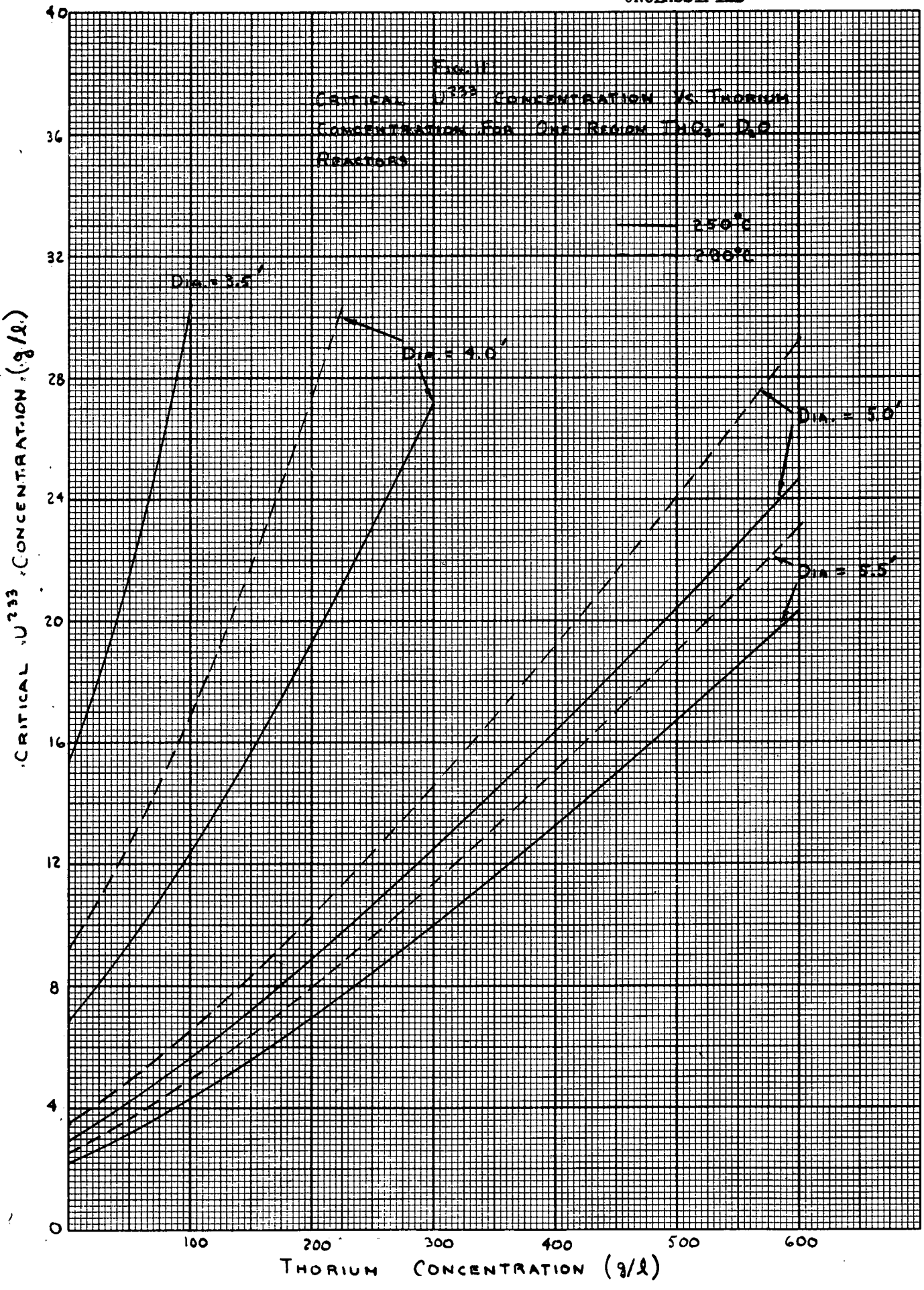

ORNL-LR-Dwg.-32416
UNCLASSIFIED

FIG. 12
CRITICAL MASS RATIO VS. THORIUM CONCENTRATION FOR ONE-REGION ThO_2-D_2O REACTORS, FUELED WITH U^{233}

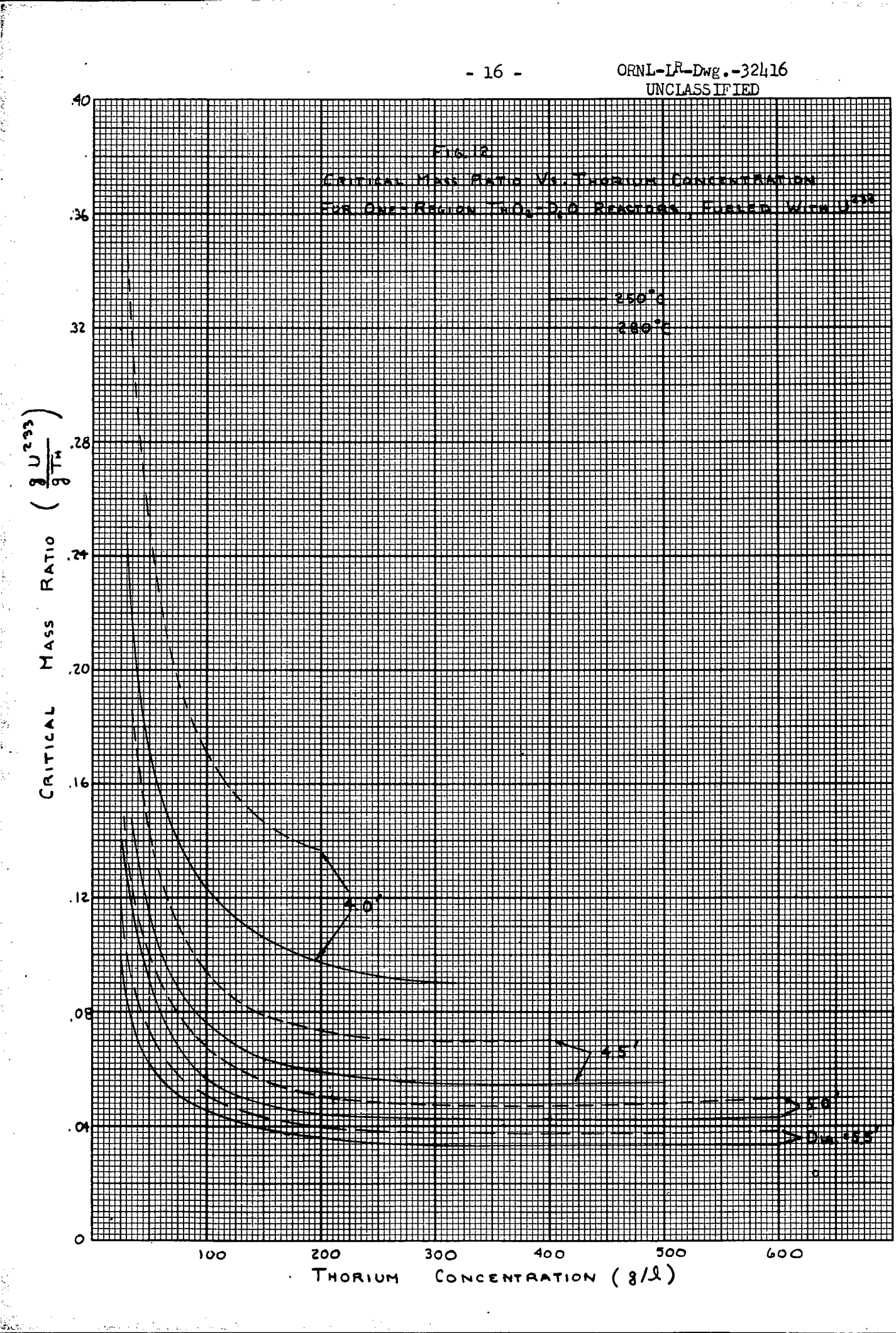

ORNL-LR-Dwg.-32417
UNCLASSIFIED

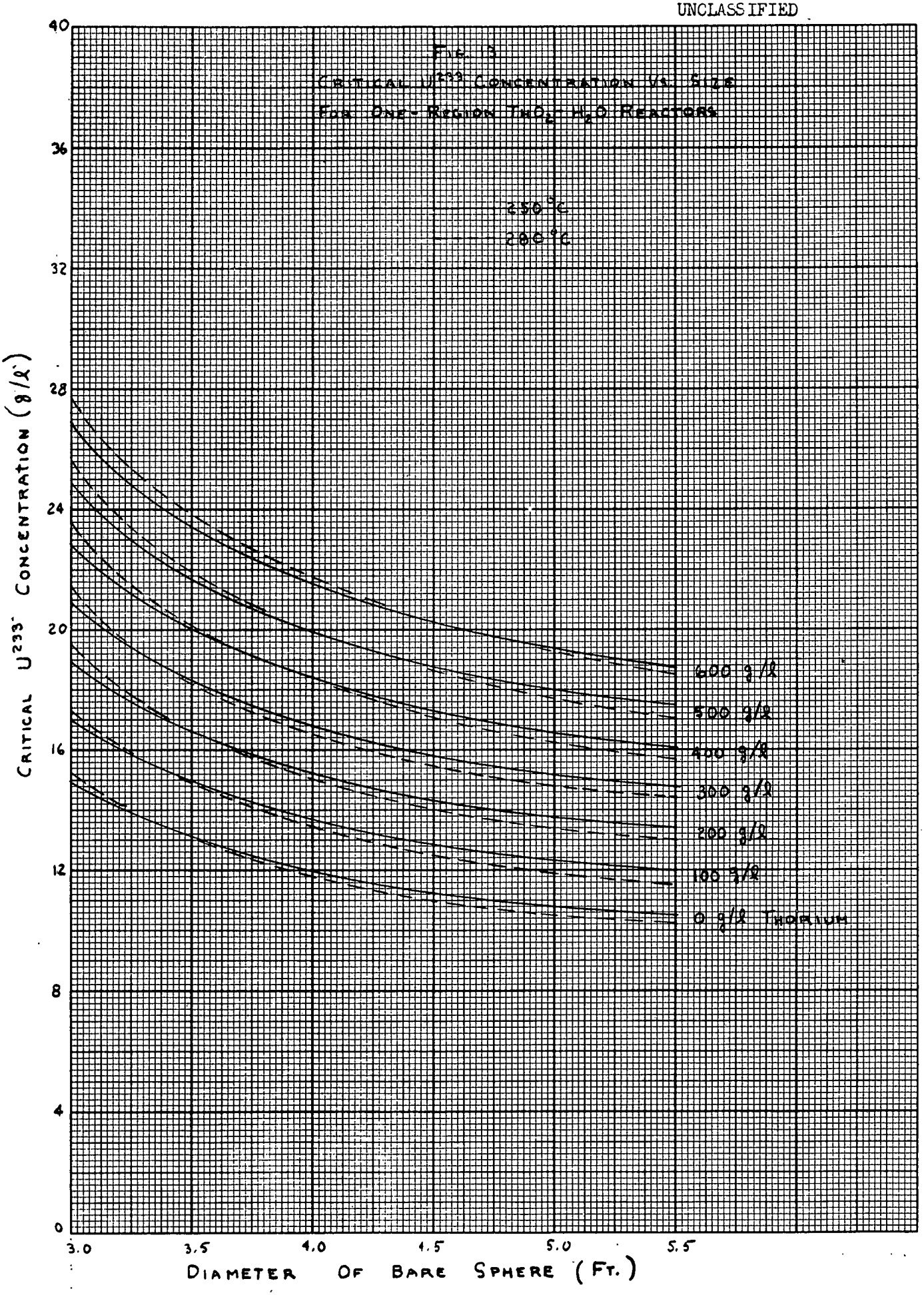

ORNL-LR-Dwg.-32418
UNCLASSIFIED

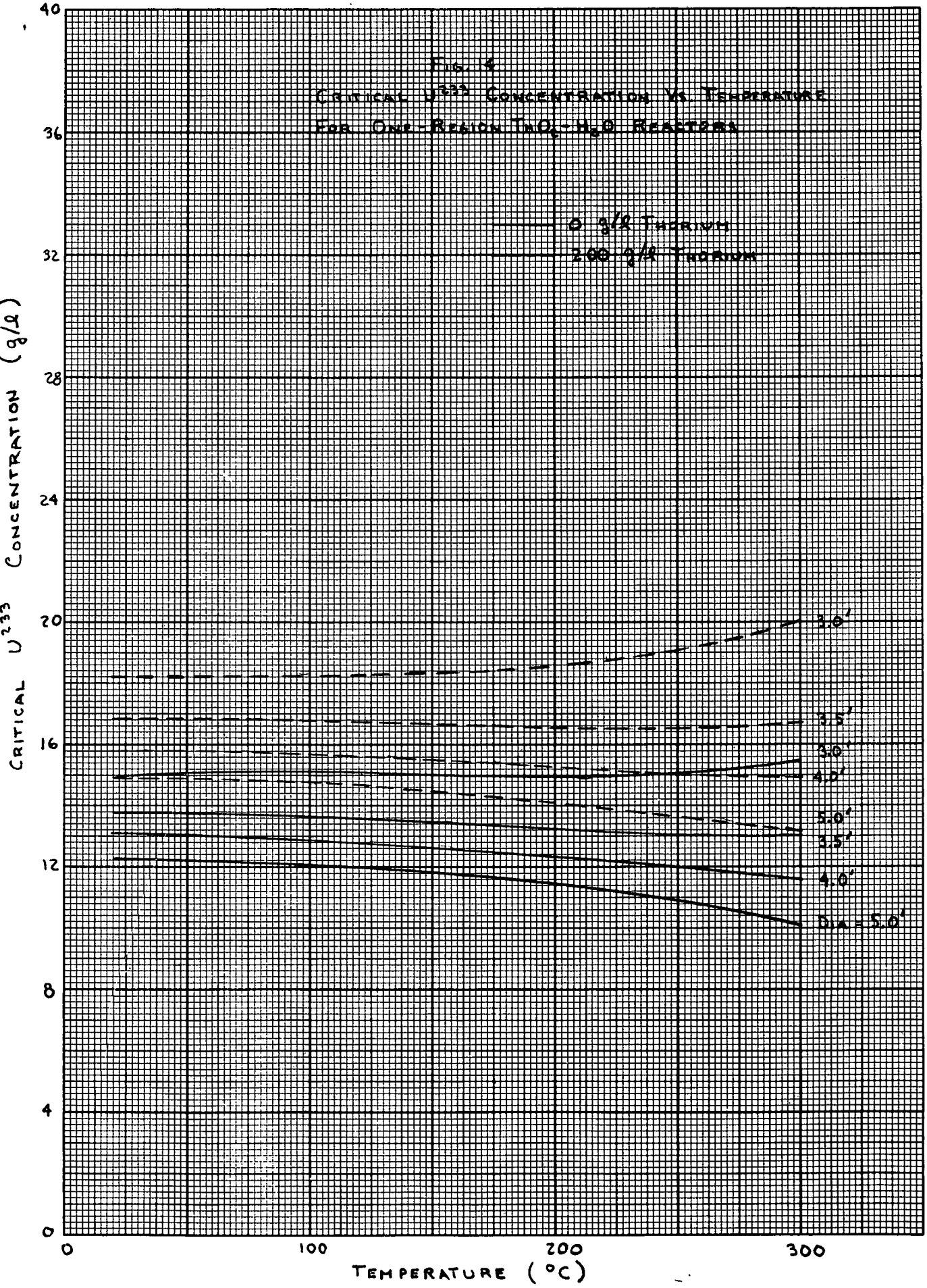

Fig. 8
Critical U^{233} Concentration Vs. Temperature
For One-Region ThO_2-H_2O Reactors

ORNL-LR-Dwg.-32419
UNCLASSIFIED

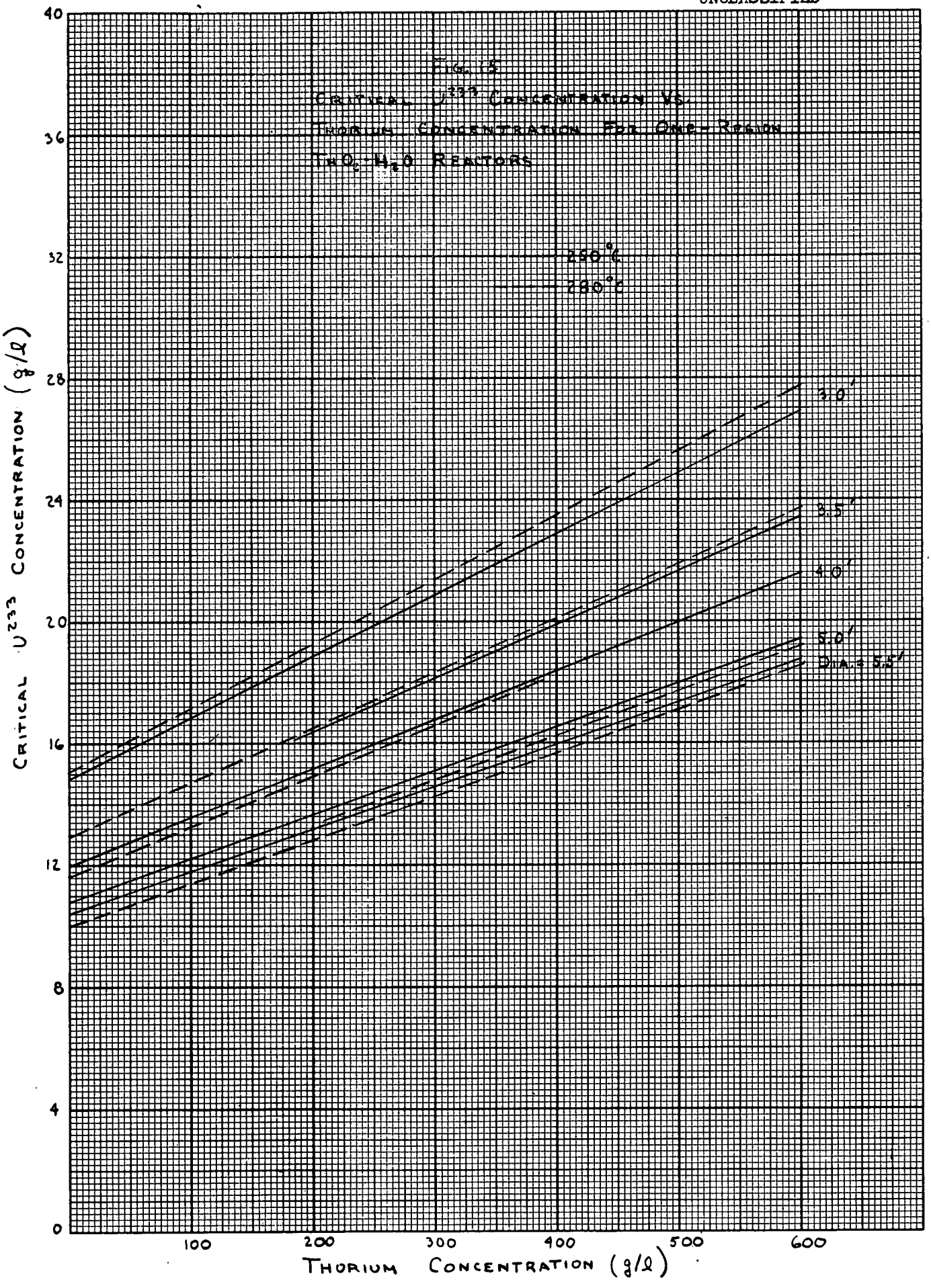

Fig. 5
Critical U^{233} Concentration vs. Thorium Concentration for One-Region ThO_2-H_2O Reactors

ORNL-LR-Dwg.-32420
UNCLASSIFIED

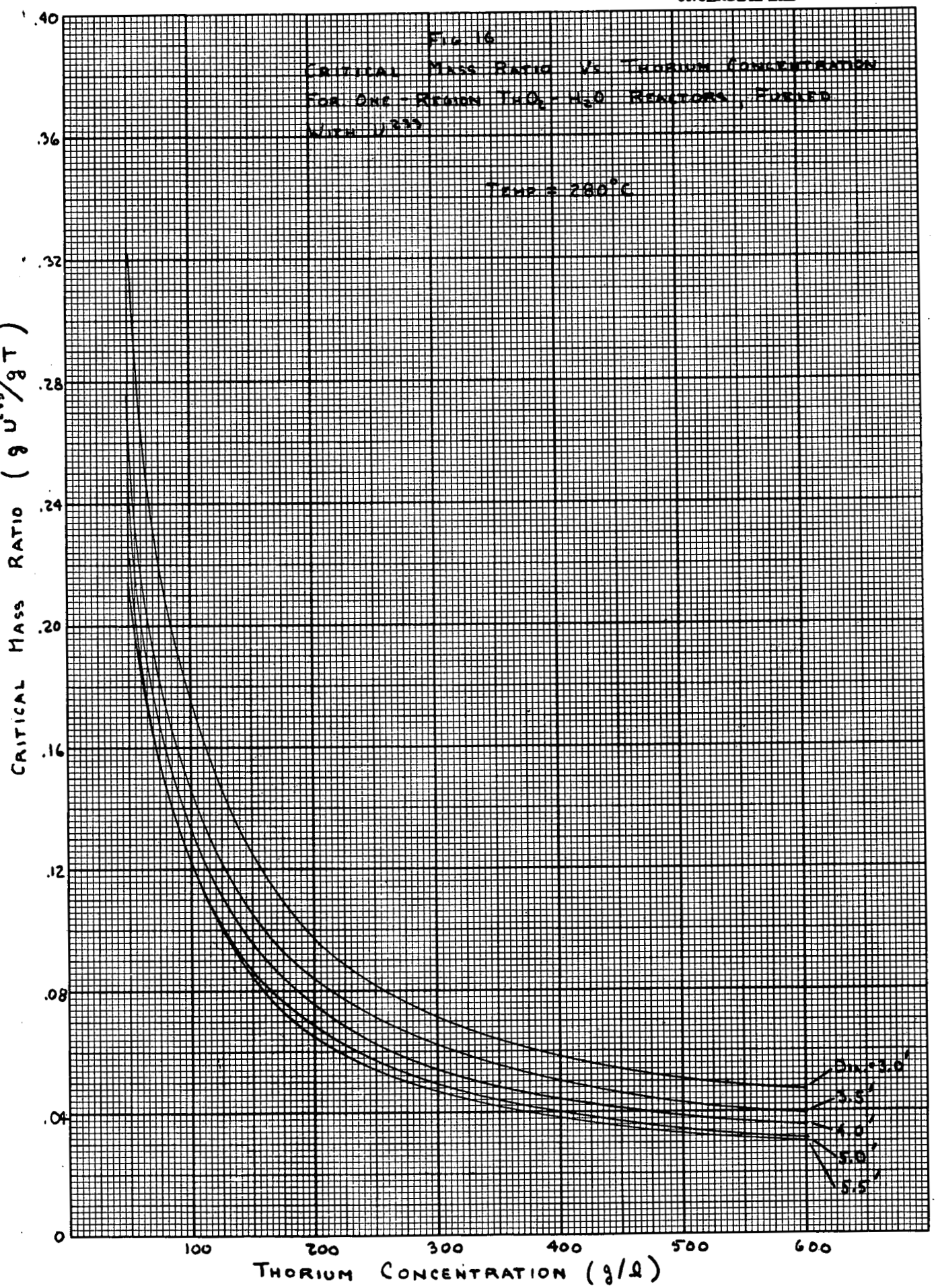

ORNL-LR-Dwg.-32421
UNCLASSIFIED

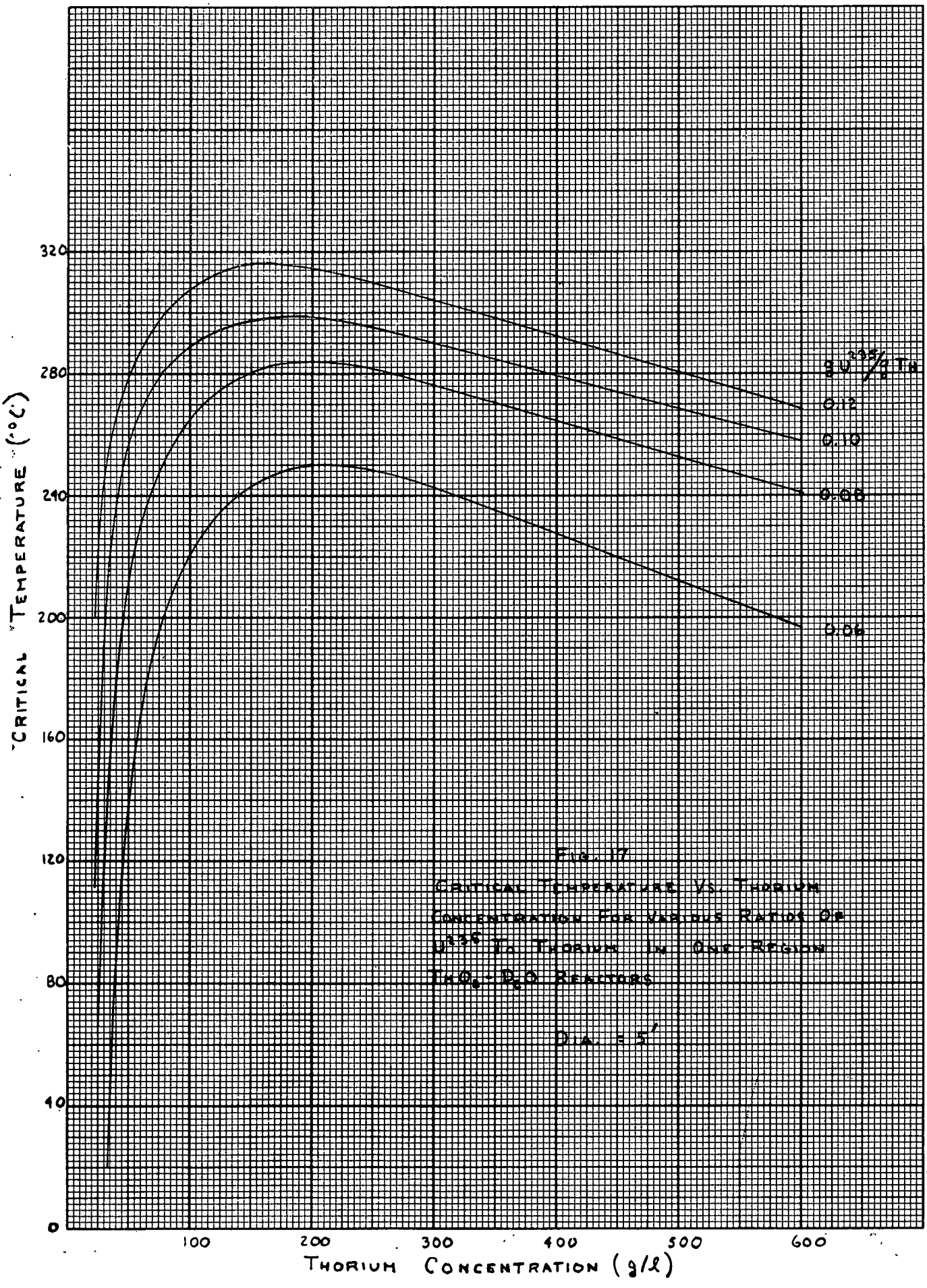

FIG. 17
CRITICAL TEMPERATURES VS. THORIUM CONCENTRATION FOR VARIOUS RATIOS OF U^{235} TO THORIUM IN ONE-REGION ThO_2-D_2O REACTORS
DIA. = 5'

ORNL-LR-Dwg.-32422
UNCLASSIFIED

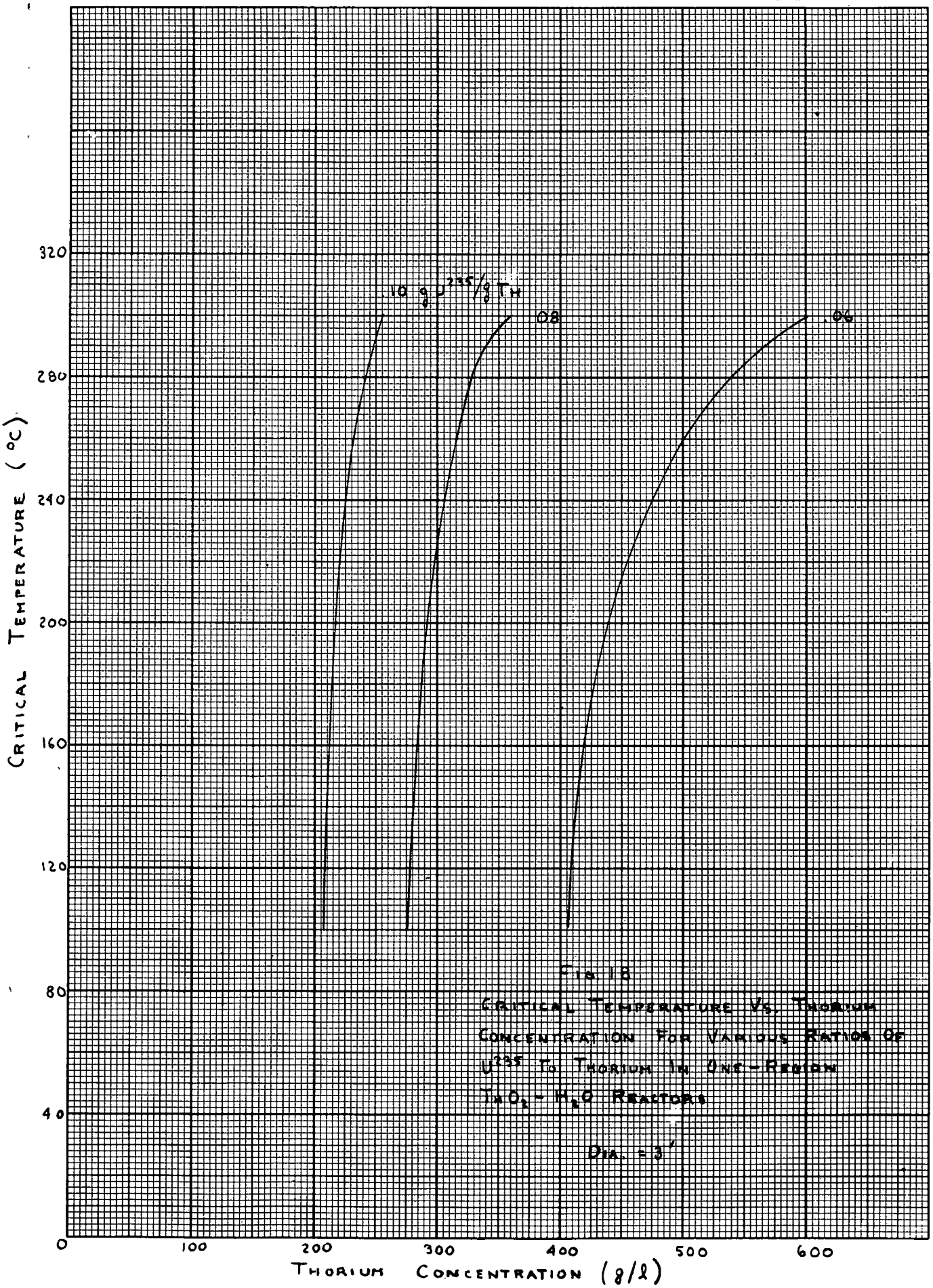

Fig. 18
Critical Temperature Vs. Thorium Concentration For Various Ratios Of U^{235} To Thorium In One-Region ThO_2 - H_2O Reactors
Dia. = 3'

ORNL-LR-Dwg.-32423
UNCLASSIFIED

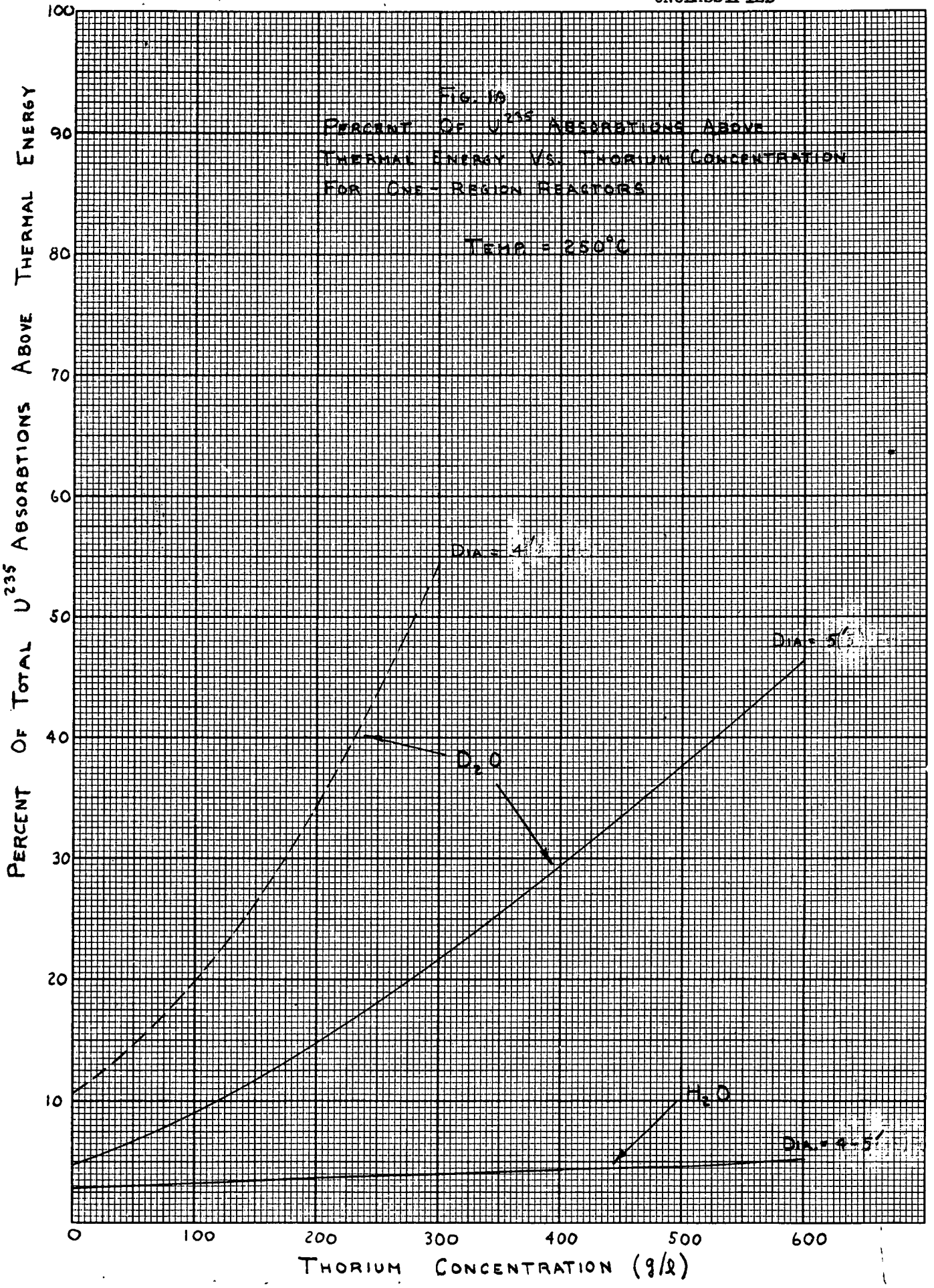

Fig. 19
Percent Of U^{235} Absorbtions Above Thermal Energy Vs. Thorium Concentration For One-Region Reactors
Temp. = 250°C

ORNL-LR-Dwg.-32424
UNCLASSIFIED

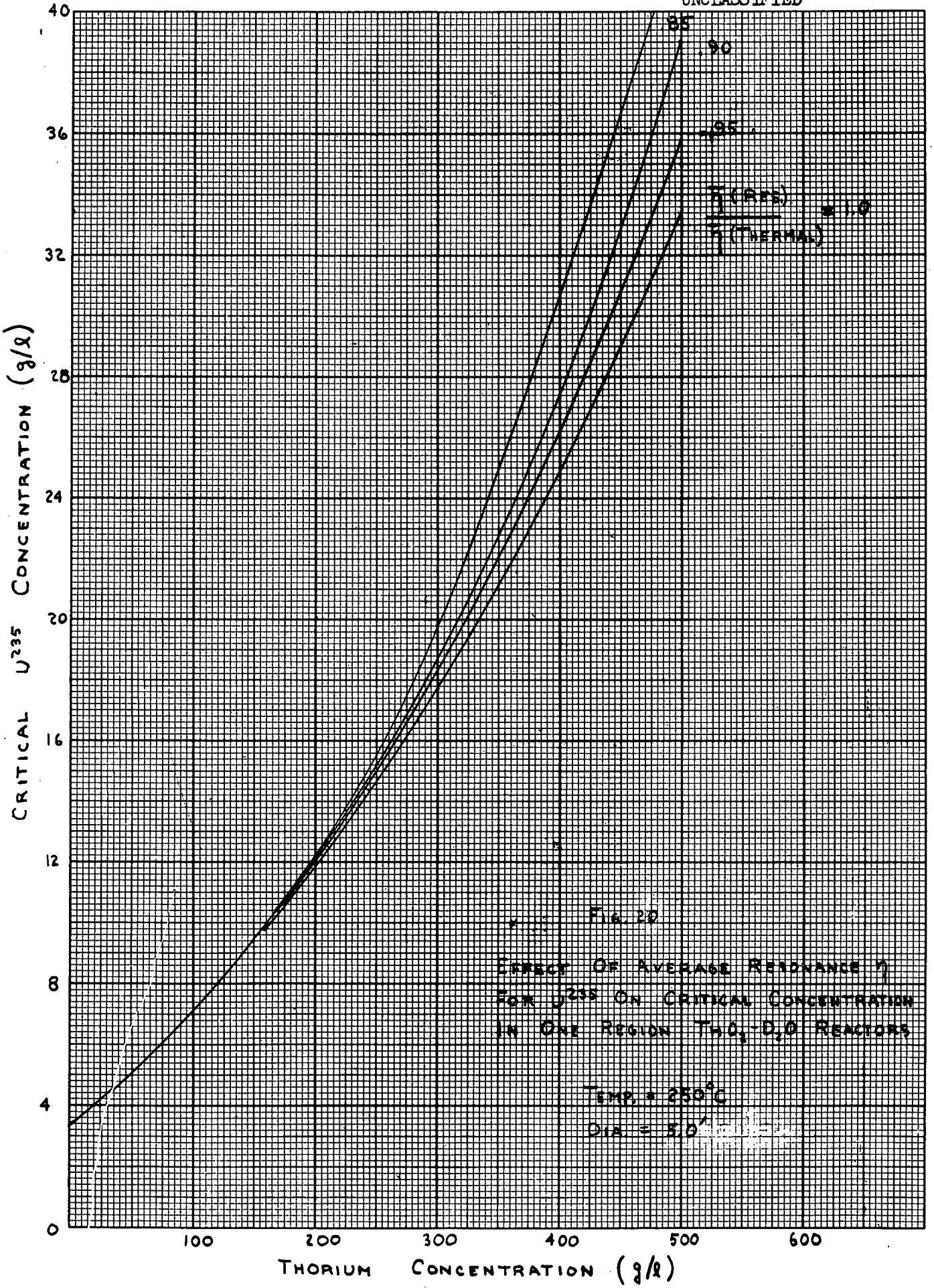

FIG. 20

EFFECT OF AVERAGE RESONANCE η FOR U^{235} ON CRITICAL CONCENTRATION IN ONE REGION ThO_2-D_2O REACTORS

TEMP. = 250°C

DIA. = 5.0'

ORNL-LR-Dwg.-32425
UNCLASSIFIED

FIG. 21
COMPARISON OF MODELS FOR CALCULATING FAST LEAKAGE FROM SMALL D_2O REACTORS

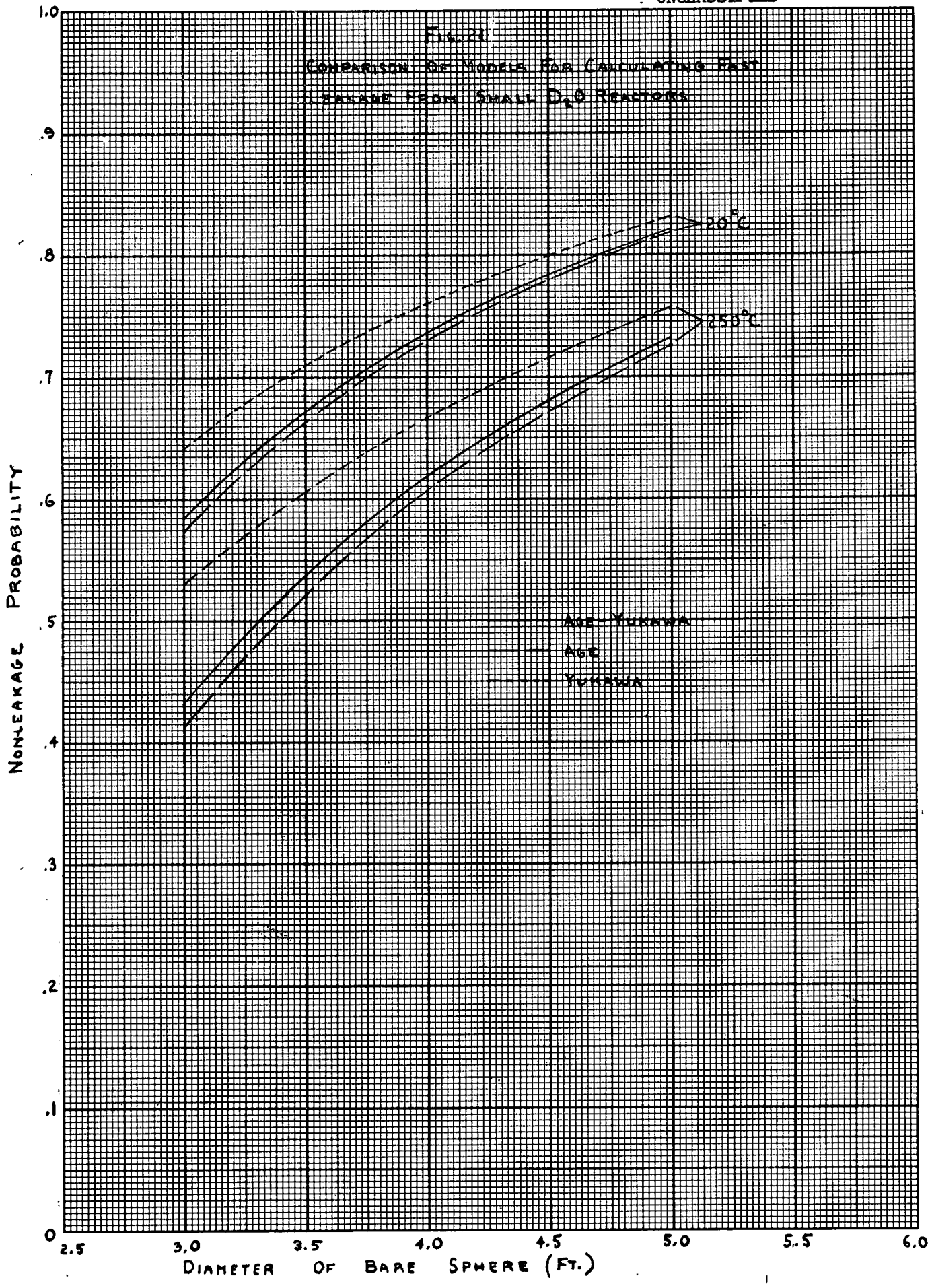

ORACLE, using a section of the nuclear code "Cornpone." Twenty fast groups, one thermal group, and two space regions (core and pressure vessel) were employed. Table III summarizes the "Cornpone" critical mass ratios for the reactors studied; as shown, at 200 g Th/liter, the critical ratio obtained for the bare 5-ft reactor using the simple model compares favorably with that obtained from the multigroup calculation. However, the comparison becomes poorer at higher slurry concentrations, due to the inadequate treatment of resonance fissions with the simplified model. In the higher concentration ThO_2-D_2O systems of the sizes studied, a significant fraction of the fissions occur above thermal energies (see Figure 18).

The increase in the effective size of the core from neutrons reflection by the pressure vessel may be estimated for the reactors listed in Table III. For example, utilizing the results in Table III and Figure 1, it is seen that approximately 10 in. should be added to the diameter of a 4- 1/2-ft I.D. pressure-vessel-enclosed D_2O reactor to obtain the diameter of the equivalent bare sphere.

Table III. Critical Mass Ratios for "Bare" and Pressure-Vessel-Enclosed Reactors at 280°C

Core Dia (ft)	Conditions	Thorium Conc. (g/liter)	"Multigroup" (g U^{235}/g Th)	"Modified Age" (g U^{235}/g Th)
5	Bare	200	0.077	0.078
		400	.141	.100
4.5	4-in. steel shell	200	.060	
		400	.105	
4	4-in. steel shell	200	.082	
		400	.146	

The computational results are shown in Figures 1 through 20. The results may be used to examine the effect on criticality produced by uniform changes in slurry composition (addition to or removal of uranium-thorium from the moderator). A particular application of this is to examine startup conditions. Figure 17 is a cross plot of the critical temperature of a 5 ft., U^{235}-D_2O reactor vs. thorium concentration, for various critical mass ratios of uranium-to-thorium. In order to illustrate the application of this figure, consider that slurry containing a fixed ratio of U^{235} to thorium is slowly added to the reactor, initially filled with D_2O at low temperature. The reactor would remain subcritical until the minimum thorium concentration required for criticality at that ratio was reached. Then, as more thorium was added to the core, the temperature would rise in accordance with the plotted curves. If the final thorium concentration were above about 200 gm/liter, the temperature would fall again with increasing thorium concentration (due to the increase in resonance neutron captures).

An alternative startup procedure would be to heat the D_2O above the maximum critical temperature before slurry was added. The uranium-thorium mixture could then be added until the desired concentration was reached, and the temperature then lowered to obtain criticality.

Figure 18 illustrates the analogous situation for an H_2O reactor in the same range of thorium concentration. The slope of the temperature curves is much greater, in accordance with the reduction in moderator absorbtions with thorium addition. Also, due to the increased moderating characteristics of the H_2O, the amount of resonance capture in thorium is less sensitive to concentration. The curves tend to level off at concentrations higher than 600 gms thorium per liter.

The D_2O-moderated reactors (in the size range considered) have a large epithermal effect compared to the H_2O systems. A comparison of the relative number of epithermal absorptions in fuel is shown in Figure 19 for both systems. The addition of thorium to the reactor has the effect of depressing the thermal flux relative to the total fast flux, and thus increases the epithermal effect.

To allow for the effect of resonance fuel absorptions on the critical concentration, an average value of η for the resonance region is required. The ratio of η-resonance to η-thermal for U^{235} in a 1/E flux was estimated by computing the ratio of resonance fission and absorption integrals from the cross-section data in BNL-325.[3] A value of 0.9 was obtained. Since the cross section of U^{233} over parts of the resonance region is uncertain, this method will not yield reliable values for U^{233}; therefore, a value of 0.95 was assumed after examination of the available data. The eta ratio was treated as a parameter in some calculations to determine its importance; the critical concentration was found to be fairly insensitive to the value used in the range of thorium concentrations considered, as shown in Figure 20.

In Figures 6 and 14 the minima in some of the curves is a result of the reduction in H_2O absorptions (as the temperature is increased) along with the increase in fast neutron leakage. It should be pointed out that this does not constitute a positive temperature coefficient, since a temperature increase would result in the removal of fuel along with the moderator.

The temperature coefficients in Table II were calculated assuming that the ratio of fuel and thorium to moderator remained constant during a thermal expansion. Changes in the bare reactor extrapolation distances were also neglected. It may be noted that the D_2O and H_2O systems differ mainly in the temperature coefficient of fast leakage.

For a temperature change which follows the spatial pattern of the power density, such as might occur during a rapid heating, the temperature coefficients in Table II should be multiplied by a weight factor accounting for the differing amounts of expansion throughout the core. For spheres, this factor is approximately equal to 2.

METHOD OF STUDY

a. Criticality Calculations:

In calculating the critical concentrations, the systems were approximated by bare, uniform spheres. The size of the actual vessel having the same critical concentration could then be obtained by subtracting an extrapolation distance from the bare sphere radius. Neglect of the vessel has the effect of simplifying the criticality equation considerably. Thus the characteristics of a large number of reactors could be surveyed in a small computing time, without the results being grossly in error.

The modified critical equation for a bare reactor is given as follows:*

$$1 = \frac{\eta_{th} \Sigma_a^{\,1} p_o p_1 g_{th}}{(\Sigma_a^{\,o} + \Sigma_a^{\,1} + \Sigma_a^{\,m})(1 + L^2 B^2)} + \eta_R \bar{p}_o (1 - p_1) g_R \qquad (1)$$

where:

η = average number of fission neutrons produced per neutron absorbed in fuel; η_{th} and η_R are the average values for the thermal region and resonance energy region ($\sim 5kT \to \infty$)

Σ_a = Macroscopic thermal absorption cross section (cm^{-1}):

superscripts o = thorium; m = moderator; 1 = fuel

L^2 = Thermal diffusion length (cm^2)

* ORACLE program written by S. Jaye and M. P. Lietzke.

B^2 = Geometric buckling (cm^{-2})

p = resonance escape probability: subscripts o = thorium; 1 = fuel; $\bar{p}_o = (1 + p_o)/2$

g = fast non-leakage probability: subscript th refers to neutrons slowing down to thermal energies, R to an average energy for resonance fission in fuel.

Equation 1 is solved by iteration for the critical fuel concentration.

The introduction of the second term on the right hand side of equation 1 is an approximation to an integral term for resonance absorption in fuel. The approximation amounts to assuming that the average of a product is a product of the averages, so that the effect on neutron cycle can be lumped into multiplicative probabilities for resonance absorption in fertile material, fuel, and fast leakage losses.

Since the resonances in fertile material and fuel overlap to a considerable extent, without going to a more involved calculation (e.g. a multigroup model) it is necessary to approximate the overall resonance structure. In these calculations, half the thorium resonances were assumed to occur at energies above and half below the energy band in which resonance absorptions in fuel occur. The further assumption was made that the average fast leakage probability to resonance fission was approximately equal to the leakage to thermal energies. In D_2O and H_2O moderated systems, with thorium concentrations in the range of interest, this assumption should introduce little error, since most of the fast leakage occurs above the low-energy resonance region. (This approximation becomes successively poorer, however, as the contribution of resonance fission to the neutron cycle becomes comparable with that from thermal fission.)

In small D_2O reactors, accurate account of fast leakage is important in calculating criticality.

Friedman and Wattenberg have found that the Fourier transform of the convolution of a Fermi age and a Yukawa, or diffusion kernel, can be used to best represent the non-leakage probability in D_2O:[2]

$$g_{\text{Indium Resonance}} = \frac{e^{-B^2\tau_1}}{1 + B^2\tau_2} \qquad (2)$$

$$\text{At } 20^\circ\text{C: } \tau_1 = 58 \text{ cm}^2, \tau_2 = 48\text{cm}^2$$

Edlund and Wood have applied the above to the calculation of criticality in the Homogeneous Reactor Test.[4] Following their procedure, an increment of 14 cm^2 was added to τ_1 to represent the age from indium resonance (1.44 ev) to thermal, so that the final values of τ in the "Age" and "Yukawa" kernels were in the ratio of 3:2, respectively. This ratio was assumed to be independent of temperature. For the reactor sizes studied, a comparison of the various approximations for the nonleakage probability is given in Figure 21. In this range, it is seen that the above expression does not differ appreciably from the Fermi slowing down model, but deviates markedly from the representation of the fast group by a single diffusion kernel.

For H_2O reactors of the same size as the D_2O systems (3-6 ft), the non-leakage probability is much larger and less sensitive to the model used to calculate the slowing down. In these calculations, a single Yukawa kernel $(1 + B^2\tau)^{-1}$ was found to closely approximate the experimental values of Hill, Roberts, and Fitch.*

---

* See reference 5, Chapter 11.

The resonance escape probability was calculated from the formula:

$$p \doteq \exp\left[-\frac{N}{\xi \Sigma_s} R_a\right] \qquad (3)$$

where N = number of atoms of resonance absorber per cm^3

Σ_s = Macroscopic scattering cross section of slurry (cm^{-1})

ξ = Average lethargy increment per collision

R_a = Effective resonance integral (barns); $R_a(\infty)$ = infinite dilution integral

Superscripts o = thorium; 1 = fuel.

for Thorium 232: [6]

$$R_a^o = 8.33\left(\frac{\Sigma_s}{N^o}\right)^{.253} \qquad o \leq \frac{\Sigma_s}{N^o} \leq 4000 \qquad (4a)$$

$$R_a^o = R_a^o(\infty) = 69.8 \qquad \frac{\Sigma_s}{N^o} > 4000 \qquad (4b)$$

for U^{235} and U^{233}:*

$$R_a^1 = 2R_a^1(\infty) = \left[\sqrt{(1+\beta)\beta} - \beta\right] \qquad o \leq \frac{\Sigma_s}{N} \leq \infty \qquad (5)$$

$$\beta = \left(\frac{0.1\pi}{R_a^1(\infty)} \quad \frac{\Sigma_s}{N^1}\right)$$

The infinite dilution fission integrals $R_f^1(\infty)$ for U^{235} and U^{233} were obtained by numerical integration of the fission cross sections in BNL-325.** As the average ratio of resonance-to-thermal η was treated as a parameter in the calculations, the value of $R_a^1(\infty)$ could then be derived, since ν is approximately constant over most of the resonance region:

---

* Due to L. Dresner (unpublished).

** These values are listed in the appendix.

$$\frac{R_f^{1}(\infty)}{R_a^{1}(\infty)} = \frac{\overline{\eta_R}}{\eta_{th}} \quad \frac{\eta_{th}}{\nu} \qquad (6)$$

In these calculations, the small contribution due to fast fissions in thorium was neglected.

---

b. Temperature Coefficients:

To compute the reactor temperature coefficients, the resonance term in equation 1 was combined with the term for thermal fission, so that the criticality formula could be written as:

$$k = \eta_{th} \epsilon p f g P \qquad (7)$$

where k = effective multiplication constant

ϵ = "fast effect," or number of neutrons from fissions at all energies, per thermal fission

f = thermal utilization

P = thermal nonleakage probability = $(1 + L^2B^2)^{-1}$

Differentiating the logarithm of equation 7 with respect to temperature gives:

$$\alpha \equiv \frac{1}{k}\frac{dk}{dT} = \frac{1}{p}\frac{dp}{dT} + \frac{1}{\epsilon}\frac{d\epsilon}{dT} + \frac{1}{f}\frac{df}{dT} + \frac{1}{g}\frac{dg}{dT} + \frac{1}{P}\frac{dp}{dT} \qquad (8)$$

For temperature changes and expansions in which the ratio of fuel and thorium to moderator remains constant, the first three terms in equation 8 are either zero or may be neglected compared to the temperature coefficients of leakage. For an increment in temperature which is spatially uniform over the reactor:

$$\frac{1}{g}\frac{dg}{dT} = -B^2\tau\left[\frac{1}{\tau}\frac{d\tau}{dT}\right] \quad \text{if } g = e^{-B^2\tau} \qquad (9a)$$

$$= -(1-g)\left[\frac{1}{\tau}\frac{d\tau}{dT}\right] \text{ if } g = \frac{1}{1+B^2\tau} \qquad (9b)$$

$$\frac{1}{\tau}\frac{d\tau}{dT} \simeq \frac{-2}{\rho}\frac{d\rho}{dT} \qquad (10)$$

where ρ is the density of the moderator.

$$\frac{1}{P}\frac{dP}{dT} \simeq \frac{-L^2B^2}{1 + L_o^2B^2 + \dfrac{\Sigma_a^o + \Sigma_a^1}{\Sigma_a^m}}\left[\frac{1}{L_o^2}\frac{dL_\rho^2}{dT}\right] \qquad (11)$$

where L_o^2 is the diffusion length in the pure moderator.

If the expansion due to a temperature change is considered to follow the space distribution of reactor power, the reactivity change should be weighted with the statistical weight of the region. Since this is equal to ϕ^2 for a one region system;

$$\frac{\delta k}{k} = \frac{\int_{\text{reactor}} \alpha\,\delta T\,\phi^2 dv}{\int_{\text{reactor}} \phi^2 dv} = \alpha\overline{\sigma\tau}\left[\frac{\int_{\text{reactor}} \phi^3 dv}{\overline{\phi}\int_{\text{reactor}} \phi^2 dv}\right] \qquad (12)$$

where $\overline{\phi}$ is the average flux in the reactor.

For a sphere in which the flux is proportional to $\frac{\sin Br}{Br}$, the factor in brackets in the above equation is approximately equal to 2.

Appendix

NUCLEAR DATA

The values of nuclear constants used in the calculations are listed in Tables IV - VII below. Except where otherwise indicated, the constants are taken from reference 6.

TABLE IV: Thermal Absorption Cross Sections (barns)*

Temperature (°C)	U^{235}	U^{233}	Thorium	H_2O
20	595	526	6.60	.586
100	515	460	5.85	.518
200	449	410	5.20	.457
250	430	385	4.94	.434
280	411	376	4.81	.424
300	402	371	4.72	.420

* Average over a Maxwell-Boltzman Distribution.

TABLE V: Age of Fission Neutrons in Mixtures of ThO_2 in D_2O and H_2O*

$\overline{\xi\sigma_s}$ (D_2O) = 5.37

$\overline{\xi\sigma_s}$ (H_2O) = 40.46

$\overline{\xi\sigma_s}$ (ThO_2) = 1.020

Temperature (°C)	Moderator	τ (cm^2) Thorium Concentration (g/liter) 0	200	400	600
20	D_2O	118	119.5	121	123
	H_2O	33	33.6	34.2	34.7
100	D_2O	129	131	132	134
	H_2O	35.6	35.9	36.2	36.6
200	D_2O	159	160	161	163
	H_2O	43.6	44.2	44.8	45.4
250	D_2O	188	189	190	191
	H_2O	50.8	51.4	51.9	52.5
280	D_2O	212	212	212	212
	H_2O	57.9	58.5	59.0	59.4
300	D_2O	236	236	236	236
	H_2O	65.1	65.6	66.1	66.5

* Based on numerical integration calculations by Tobias (Ref., 6 and additional private communications.)

TABLE VI: Thermal Diffusion Coefficients in D_2O and H_2O* (cm)

Temperature	Moderator	D (cm) Thorium Concentration 0	200	400	600
20	D_2O	.825	.825	.825	.825
	H_2O	.160	.163	.166	.169
100	D_2O	.905	.900	.894	.890
	H_2O	.177	.179	.182	.186
200	D_2O	1.047	1.037	1.026	1.017
	H_2O	.218	.221	.225	.228
250	D_2O	1.160	1.145	1.130	1.116
	H_2O	.246	.250	.254	.258
280	D_2O	1.245	1.225	1.205	1.190
	H_2O	.267	.271	.275	.279
300	D_2O	1.320	1.298	1.277	1.255
	H_2O	.282	.287	.290	.294

* The coefficients for H_2O are approximate values calculated from the cross sections for H_2O reported in BNL-325.

TABLE VII: Fission Integrals at Infinite Dilution* (barns)

Temperature	U^{235}	U^{233}
20	530	1067
100	477.5	1012
200	434	966
250	412.5	943
280	402.5	933
300	395.0	927

* Obtained by numerical integration of the fission cross sections reported in BNL-325.

REFERENCES

1. J. H. Alexander and N. D. Given; A Machine Multigroup Calculation, ORNL-1925, September 6, 1955.

2. F. L. Friedman and A. Wattenberg; Age of Fission Neutrons in D_2O, CP-3453, March 6, 1946.

3. D. J. Hughes and J. A. Harvey; Neutron Cross Sections, BNL-325, July 1, 1955.

4. M. C. Edlund and P. M. Wood; Physics of the Homogeneous Reactor Test, ORNL-1780, August 27, 1954.

5. A. M. Weinberg and E. P. Wigner; Theory of Neutron Chain Reactions, University of Chicago Press (to be published).

6. T. B. Fowler and M. Tobias; Two-Group Constants for Aqueous Homogeneous Reactor Calculations, ORNL CF 58-1-79, January 22, 1958.

DISTRIBUTION

1. HRP Director's Office Rm. 259, Bldg. 9204-1
2. G. M. Adamson
3. S. E. Beall
4. L. L. Bennett
5. A. M. Billings
6. E. G. Bohlmann
7. J. C. Bolger
8. S. E. Bolt
9. E. S. Bomar
10. J. R. Brown
11. W. D. Burch
12. R. H. Chapman
13. R. Chalkley
14. R. D. Cheverton
15. H. C. Claiborne
16. E. L. Compere
17. R. S. Crouse
18. J. S. Culver
19. D. G. Davis
20. R. J. Davis
21. J. R. Engle
22. J. L. English
23. D. E. Ferguson
24. J. D. Flynn
25. T. B. Fowler
26. C. H. Gabbard
27. W. R. Gall
28. E. H. Gift
29. J. C. Griess
30. R. S. Greeley
31. P. A. Haas
32. P. H. Harley
33. P. N. Haubenreich
34. J. W. Hill
35. E. C. Hise
36. C. J. Hochanadel
37. S. Jaye
38. G. H. Jenks
39. D. T. Jones
40. S. I. Kaplan
41. P. R. Kasten
42. F. Kertesz
43. J. O. Kolb
44. R. B. Korsmeyer
45. K. A. Kraus
46. C. G. Lawson
47. R. E. Leuze
48. M. P. Lietzke
49. R. A. Lorenz
50. M. I. Lundin
51. R. N. Lyon
52. W. L. Marshall
53. T. Mauney
54. J. P. McBride
55. J. F. McDuffie
56. H. A. McLain
57. R. A. McNees
58. J. R. McWherter
59. R. L. Moore
60. C. S. Morgan
61. C. W. Nestor
62. L. F. Parsly, Jr.
63. F. N. Peebles
64. M. L. Picklesimer
65 - 75. B. E. Prince
76. S. A. Reed
77. D. M. Richardson
78. G. W. Rivenbark
79. R. C. Robertson
80 - 90. M. W. Rosenthal
91. H. C. Savage
92. C. L. Segaser
93. E. M. Shank
94. M. D. Silverman
95. M. J. Skinner
96. I. Spiewak
97. R. W. Stoughton
98. J. A. Swartout
99. E. H. Taylor
100. D. G. Thomas
101. D. S. Toomb
102. W. E. Unger
103. E. R. Volk
104. R. Van Winkle
105. A. M. Weinberg
106. K. W. West
107. J. C. Wilson
108. C. E. Winters
109. F. C. Zapp
110 - 111. REED Library
112 - 113. Central Research Library
114 - 128. Laboratory Records
129. ORNL-RC

EXTERNAL

130. F. C. Moesel, AEC, Washington
131 - 137. Westinghouse PAR Project
138 - 152. TISE-AEC